Iron Bioavailability and Redox Activity in Diverse Carbon Nanotube Samples

Lin Guo,[†] Daniel G. Morris,[†] Xinyuan Liu,[‡] Charles Vaslet,[§] Robert H. Hurt,[†] and Agnes B. Kane*[,§]

Division of Engineering, Department of Chemistry, and Department of Pathology and Laboratory Medicine, Brown University, Providence, Rhode Island 02912

Received November 12, 2006. Revised Manuscript Received February 18, 2007

The ultimate success of many nanotechnologies will depend on our ability to understand and manage nanomaterial health risks. Carbon nanotubes are now primarily fabricated by catalytic routes and typically contain significant quantities of transition metal catalyst residues. Iron-catalyzed free-radical generation has been hypothesized to contribute to oxidative stress and toxicity upon exposure to ambient particulate, amphibole asbestos fibers, and single-wall carbon nanotubes. A key issue surrounding nanotube iron is bioavailability, which has not been systematically characterized, but is widely thought to be low on the basis of electron microscope observations of metal encapsulation by carbon shells. Here, we validate and apply simple acellular assays to show that toxicologically significant amounts of iron can be mobilized from a diverse set of commercial nanotube samples in the presence of ascorbate and the chelating agent ferrozine. This mobilized iron is redox active and induces single-strand breaks in plasmid DNA in the presence of ascorbate. Iron bioavailability varies greatly from sample to sample and cannot be predicted from total iron content. Iron bioavailability is not fully suppressed by vendor "purification" and is sensitive to partial oxidation, mechanical stress, sample age, and intentional chelation. The results suggest practical materials chemistry approaches for anticipating and managing bioavailable iron to minimize carbon nanotube toxicity.

Introduction

Carbon nanotubes (CNTs) are being manufactured in ever larger quantities, and concerns about human health risks have led to a rapidly growing literature on their potential toxicity.[1−7] The studies to date show wide variability in biological responses to nanotubes, and we hypothesize that one contributing factor is real sample-to-sample variability in nanotube material properties. Carbon nanotubes are best regarded as a family of materials with wide variation and distribution in tube diameter (wall number), length, carbon surface chemistry, and metallic impurities,[8] which most commonly include Fe, Ni, Y, or Co. Catalytically synthesized carbon nanotubes typically contain 3−30 wt % metal as produced, whereas most commercially "purified" products contain lower but significant amounts of metal residue (1.2−10.9% in our sample set).

The current study focuses on iron, which has been hypothesized to contribute to the toxicity of ambient ultrafine particles,[9] amphibole asbestos fibers,[10−12] and Fe-containing single-walled nanotubes (SWNTs).[3,4] Ambient fine ($<2.5\ \mu$m) and ultrafine particles ($\leq$100 nm), which, like nanotubes, contain graphenic (sp^2-hybridized) elemental carbon, also contain transition metals, as well as hydrocarbons, quinones, and bacterial endotoxin.[9] Epidemiologic studies have confirmed that ambient air pollution particles are associated with adverse health effects in susceptible populations.[9,13] It is postulated that the high surface area of ambient ultrafine particles, as well as engineered carbon nanomaterials, can catalyze generation of reactive oxygen species, especially in the presence of transition metal contaminants such as iron that participate in redox cycling reactions.[14]

Iron in carbon nanotubes has been reported to be a mixture of α-Fe^0, γ-Fe^0, and carbide phases[15] and much of the metal appears by TEM to be at least superficially encapsulated by carbon.[15−17] The key question for the possible biological

* Corresponding author. Brown University, Box G-E5, Providence, RI 02912-G. Tel: (401) 863-1110, Fax: (401) 245-9432. E-mail: Agnes_Kane@brown.edu.
[†] Division of Engineering, Brown University.
[‡] Department of Chemistry, Brown University.
[§] Department of Pathology and Laboratory Medicine.

(1) Smart, S. K.; Cassady, A. I.; Lu, G. Q.; Martin, D. J. *Carbon* **2006**, *44*, 1034−1047.
(2) Lam, C.; James, J. T.; McCluskey, R.; Hunter, R. L. *Toxicol. Sci.* **2004**, *77*, 126−134.
(3) Shvedova, A. A., et al. *J. Toxicol. Environ. Health, Part A* **2003**, *66*, 1909−1926.
(4) Kagan, V. E., et al. *Toxicol. Lett.* **2006**, *165* (1), 88−100.
(5) Warheit, D. B., et al. *Toxicol. Sci.* **2004**, *77*, 117−125.
(6) Monteiro-Riviere, N. A.; Nemanich, R. J.; Inman, A. O.; Wang, Y. Y.; Riviere, J. E. *Toxicol. Lett.* **2005**, *155*, 377−384.
(7) Sayes, C. M., et al. *Toxicol. Lett.* **2006**, *161* (2), 135−142.
(8) Moisala, A.; Nasibulin, A. G.; Kauppinen, E. I. *J. Phys. Condens. Matter* **2003**, *15*, 3011−3035.
(9) Tao, F.; Gonzalez-Flecha, B.; Kobzik, L. *Free Radical Biol. Med.* **2003**, *35*, 327−340.
(10) Fubini, B.; Areán, C. O. *Chem. Soc. Rev.* **1999**, *28*, 373−381.
(11) Hardy, J. A.; Aust, A. E. *Chem. Rev.* **1995**, *95*, 97−118.
(12) Donaldson, K.; Aitken, R.; Tran, L.; Stone, V.; Duffin, R.; Forrest, G.; Alexander, A. *Toxicol. Sci.* **2006**, *91*, 5−22.
(13) Oberdörster, G.; Oberdörster, E.; Oberdörster, J. *Environ. Health Perspect.* **2005**, *113*, 823−839.
(14) Nel, A.; Xia, T.; Mädler, L.; Li, N. *Science* **2006**, *311*, 622−627.
(15) Kim, H.; Sigmund, W. *Carbon* **2005**, *43*, 1743−1748.
(16) Lam, C.; James, J. T.; McCluskey, R.; Arepalli, S.; Hunter, R. L. *Crit. Rev. Toxicol.* **2006**, *36*, 189−217.

10.1021/cm062691p CCC: $37.00
Published on Web 06/09/2007

reactivity of these iron residues is whether some portion of the metal is accessible (or can be rendered accessible by processing) to water chelating agents and reductants in biological media and thus able to participate in redox reactions generating reactive oxygen species that are the molecular basis of cellular iron toxicity.[18]

In the emerging nanotoxicology literature, there is increasing awareness of the complexity of, and variability in, carbon nanotube samples, and there have been calls to accompany all toxicity studies with comprehensive materials characterization.[19,20] Unfortunately, no materials diagnostic commonly applied in carbon nanotube research provides direct information on iron bioavailability, and as a result, there are no systematic data on iron bioavailability across a range of CNT types and formulations. Here, we adapt and validate simple acellular assays for assessing the release and redox activity of CNT-iron and apply them to a range of commercial samples. We also systematically study the effect of sample age, the effect of postprocessing stresses (oxidation or mechanical grinding) that may damage the carbon shells and expose fresh metal surface, and the effect of chelation as a possible mitigation scheme.

Materials and Methods

Materials and Their Characterization. Iron-containing carbon nanotube samples were obtained from three commercial vendors in powder form and used as received except where noted. Their metals contents were determined by ICP at Huffman Analytical Laboratories (Golden, CO); in addition to Fe, they contain small amounts of other transition metals (sum of Cr, Co, Cu, Ni, V, Zn ranges from 20 to 550 ppm by ICP). X-ray diffraction spectra were acquired on a Bruker AXS D8 Advance instrument at Brown University. Iron forms were further investigated by Mössbauer spectroscopy at 77.5 K, which was carried out by William Reiff at Mössbauer Spectroscopy Consultants. Carbon nanofibers (pure and 5.7 wt % elemental Fe-doped) used as a model system were synthesized at Brown University from a discotic liquid crystalline precursor (AR mesophase, Mitsubishi Gas Chemical, <7 ppm iron and <5 ppm each Cr, Co, Cu, Ni, V, Zi by ICP) by a templating method described by Jian et al.[21] Nanophase Fe particles were doped on the carbon nanofiber surfaces by incipient wetting of iron nitrate nonahydrate solution (the weight ratio of iron to CNF is 5.7%) followed by drying and reduction in 1% H_2 in He at 700 C for 3 h. Supercoiled ϕX174 DNA (Form RFI) was obtained from New England Biolabs (Beverly, MA). The DNA was ethanol-precipitated[22] from stock buffer and dissolved in 25 mM MOPS pH 7. MOPS, sodium L-ascorbate, and deferoxamine mesylate (desferrioxamine B) were purchased from Sigma Chemical Co. (St Louis, MO). Ferrozine was obtained from Aldrich Chemical (Milwaukee, WI). Stock solutions of ascorbate, desferoxamine mesylate, and ferrozine were prepared fresh in 25 mM MOPS, pH 7, just prior to use and stored in the dark. Crocidolite asbestos (UICC Lot# 1040619) used as a reference material was obtained from Structure Probe, Inc. (West Chester, PA). Hematite (red iron oxide powder, Fe_2O_3; 1−3 μm particle size) was a gift from Atlantic Equipment Engineers (Bergenfield, NJ). Iron(III) oxide nanopowder (5−25 nm particle size) was obtained from Sigma-Aldrich, Inc. (St. Louis, MO). Carbon black was obtained from Cabot Corporation (M120 grade, <20 ppm Fe by ICP).

Fe Mobilization Assay. Solid samples (single- and multiwall carbon nanotubes, carbon nanofibers, Fe-doped carbon nanofibers, carbon black, crocidolite asbestos, and Fe_2O_3) were dispersed at 1 mg/mL in chelex-treated water by sonication for 30 min at room temperature. Dispersed materials (0.667 mg/mL) were mixed by vortexing for 30 s in 50 mM MOPs, pH 7.0, containing 1 mM ferrozine with or without 1 mM ascorbate. All samples were placed on a mini mixing machine in a dark environment. After 72 h, 1.5 mL samples were withdrawn and centrifuged at 14 000 rpm for 45 min. SWNTs were removed using a biospin disposable chromatography column at 500 rpm at 4 °C. The concentration of mobilized Fe(II)-ferrozine complex was determined by absorbance at 562 nm.

Plasmid DNA Break Assay. *Dose−Response curves:* Samples (carbon nanofibers, Fe-doped carbon nanofibers, crocidolite asbestos, carbon black, and hematite) were dispersed at 41 μg/mL in 25 mM MOPS, pH 7, by sonication for 1 h at 42 °C. For the DNA break assay, dispersed materials were incubated with 1 μg of ϕX174 RFI (supercoiled) DNA with or without 1 mM ascorbate in a 100 μL reaction volume for 1 h at 37 °C with mixing. Tracking dye was added to each assay, mixed, and centrifuged at 16 000× g to remove particulates. Duplicate samples of each assay were separated by electrophoresis in a 0.8% agarose gel containing 0.3 μg/mL ethidium bromide at 100 V for 20 min. NIH Image v1.56 software was used to analyze digitized UV trans-illuminated gel images. Integrated peak areas representing forms RFI (supercoiled) and RFII (nicked) DNA were used to determine the fraction of form RFI remaining in each lane by dividing the RFI area by the total area of RFI and RFII. Samples were compared by expressing each calculated RFI value as a percentage of a DNA-only control (treated under identical conditions) and subtracted from 100% to give the percentage of DNA with breaks. Prevention of DNA breaks by the iron chelators desferrioxamine mesylate or ferrozine was assessed by adding the chelators (1 mM) to the incubation assay. Ascorbate (1 mM) alone incubated with supercoiled DNA for 1 h at 37 °C induced breaks in 4 ± 1% of plasmid DNA. No breaks were induced in the absence of ascorbate. All DNA break assays were performed in subdued light.

DNA Break Assay for Commercial Nanotubes: Samples (unpurified carbon nanotubes, purified carbon nanotubes, purified ground carbon nanotubes, purified oxidized carbon nanotubes, and crocidolite asbestos as a reference material) were dispersed at 41 μg/mL in 25 mM MOPS, pH 7, by sonication for 1 h at 42 °C. Dispersed materials were preincubated with or without 1 mM ascorbate for 30 min at 37 °C with mixing followed by centrifugation at 24 652× g for 30 min to remove particulates. For the DNA break assay, supernatants were immediately added to 1 μg of ϕX174 RFI DNA in a 100 μL reaction volume and incubated at 37 °C for 30 min with mixing or shaking. Tracking dye was added to each assay, and duplicate samples were separated on 0.8% agarose gels and analyzed as described above.

(17) Xu, Y.; Peng, H.; Hauge, R. H.; Smalley, R. E. *Nano Lett.* **2005**, *5* (1), 163−168.
(18) Papanikolauou, G.; Pantopoulos, K. *Toxicol. Appl. Pharmacol.* **2005**, *202*, 199−211.
(19) Hurt, R. H.; Monthioux, M.; Kane, A. *Carbon* **2006**, *44*, 1028−1033.
(20) Powers, K. W.; Brown, S. C.; Krishna, V. B.; Wasdo, S. C.; Moudgil, B. M.; Roberts, S. M. *Toxicol. Sci.* **2006**, *90* (2), 296−303.
(21) Jian, K.; Shim, H.-S.; Schwartzman, A.; Crawford, G. P.; Hurt, R. H. *Adv. Mater.* **2003**, *15* (2), 164−167.
(22) Maniatis, T.; Fritsch, E. F.; Sambrook, J. *Molecular Cloning: A Laboratory Manual*; Cold Spring Harbor Laboratory: Cold Spring Harbor, NY, 1982; pp 461−462.
(23) Timbrell, V. Characteristics of the International Union Against Cancer Standard Reference Samples of Asbestos. In *Pneumoconiosis: Proceedings of the International Conference*, Johannesburg, 1969; Shapiro, H. A., Ed.; Oxford University Press: Cape Town, 1970; pp 28−36.

a

Table 1 Total Fe content of nanotube samples

Sample	Fe content (wt-%)
Unpurified MWNTs A	4.40%
Purified MWNTs A	1.21%
Oxidized purified MWNTs A	1.29%
Ground purified MWNTs A	1.21%
Unpurified MWNTs B	4.25%
Purified MWNTs B	3.29%
Unpurified SWNTs C	22.20%
Purified SWNTs C	10.90%
UICC Crocidolite Asbestos	22.20%

data from Huffman Lab by ICP-MS analysis

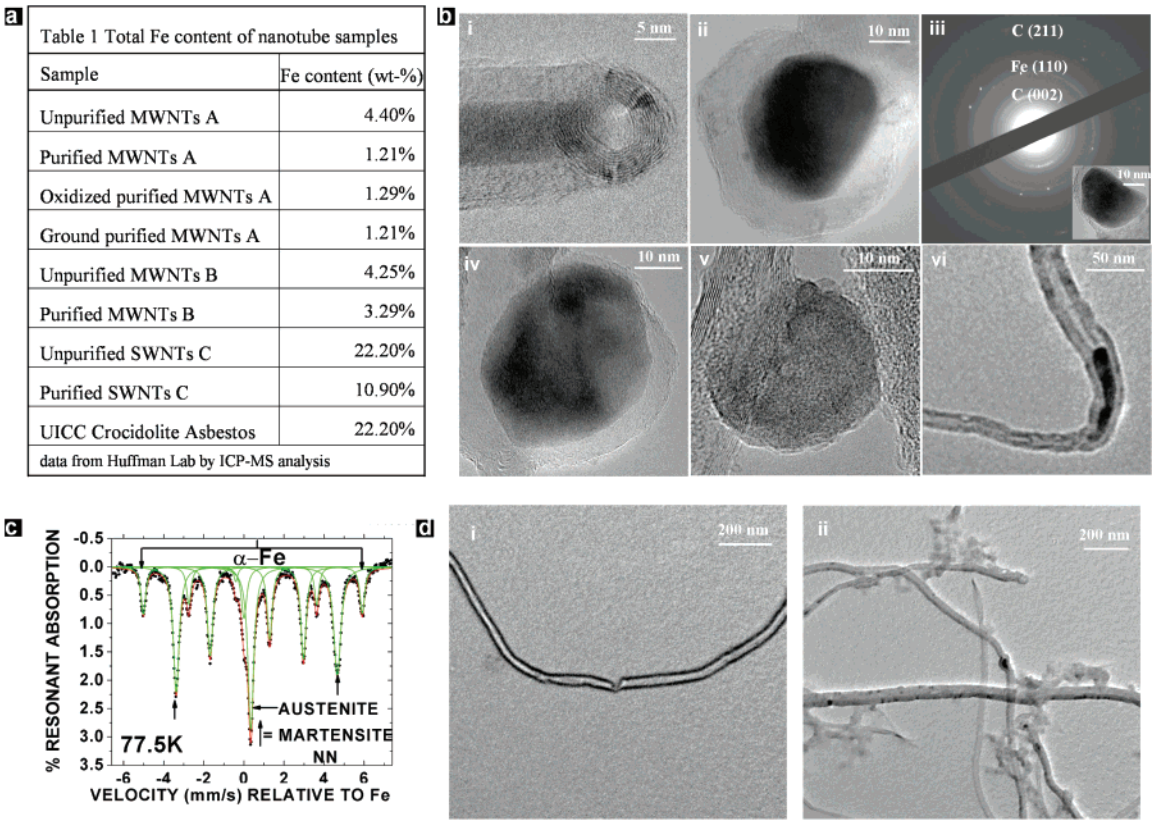

Figure 1. Iron content, morphology, and phase in catalytically produced carbon nanotubes. (a) Total elemental Fe content for a panel of commercial materials determined by ICP-atomic emission spectroscopy; (b,c) examples of Fe/C association morphologies (most common ii, iv, vi) and electron diffraction pattern and Mössbauer spectra for the as-produced MWNT A sample; (d) structural damage caused by (i) air oxidation and (ii) grinding of the purified MWNT A sample with a ceramic mortar/pestle, carried out intentionally to assess whether fresh iron can be exposed during mechanical stress or partial oxidation. Image (ii) shows that grinding leads to the collection of amorphous carbonaceous debris on the outside of the tubes. Both Mössbauer spectra and electron diffraction patterns show a predominance of reduced iron/carbon phases (α-Fe, γ-Fe, and martensite or ϵ-iron carbide), whereas electron diffraction suggests a limited amount of iron oxide [(secondary dots in b-iii are consistent with Fe_3O_4) in some locations, most likely associated with iron surface patches that are exposed to atmospheric oxygen. The asbestos reference sample is from the International Union Against Cancer (UICC) with iron content determined by neutron activation analysis.[23]

Results

For this study, we assembled a panel of six nanotube samples, comprising pairs of "as-produced" and "purified" samples from three commercial vendors. Figure 1 shows that their elemental iron content ranges from 1.2 to 22 wt %, with the latter number being similar to the iron content of the UICC crocidolite asbestos used here as a reference material. Mössbauer spectra of the vendor A samples show a dominance of reduced iron/carbon phases, including α-iron (zero-valent), the high-temperature phase austenite (γ-iron), and either martensite or epsilon iron carbide, which are typical phases observed upon quenching iron/carbon systems from high-temperature reducing environments. These iron phases are known to be thermodynamically unstable in air and susceptible to oxidative corrosion under ambient conditions. TEM analysis showed a wide range of complex Fe/C morphologies, including metal rods within nanotube channels and Fe nanoparticles partially or wholly surrounded by carbon shells of variable thickness (see examples in Figure 1b). Some of the carbon shells are amorphous, whereas others exhibit a high degree of graphenic crystalline order with well-developed 002 lattice fringes in concentric order surrounding the iron-rich core. Even high-resolution TEM characterization does not provide a clear picture of iron bioavailability, because some graphenic shells are present but quite thin (Figure 1b-iv), and others may possess defects that are not apparent in two-dimensional projection. Further, the interpretation of open CNT tips on the basis of concentric fringe structures such as Figure 1b-i is not reliable, and even iron rods deeply imbedded in the central nanotube core may have access to fluid phases through nearby wall defects, because water is known to enter nanotubes by capillary forces under some conditions.[24] We believe that reliable determination of the bioavailability of CNT catalyst residues cannot be solely on the basis of electron microscopy but requires sensitive quantitative assays for iron mobilization and redox-activity.

To assess the bioavailability of iron catalyst residues in commercial nanotubes, a mobilization assay was carried out at physiological pH using the chelator ferrozine, which binds with Fe^{2+} to form a blue complex.[11] The amount of iron mobilized from these commercial samples was increased in the presence of 1 mM ascorbate (Figure 2a) and varied from about 1 to 7% of the total Fe in the sample (Figure 2e) over the course of our 3-day assay. We used sonication to disperse the CNTs in both assays and the question arises whether this sonication was directly responsible for iron release by damaging the surrounding carbon shells. To assess this possibility, we conducted several experiments without any sonication and found similar but slightly lower concentrations

(24) Mattia, D.; Bau, H.; Gogotsi, Y. *Langmuir* **2006**, *22*, 1789−1794.

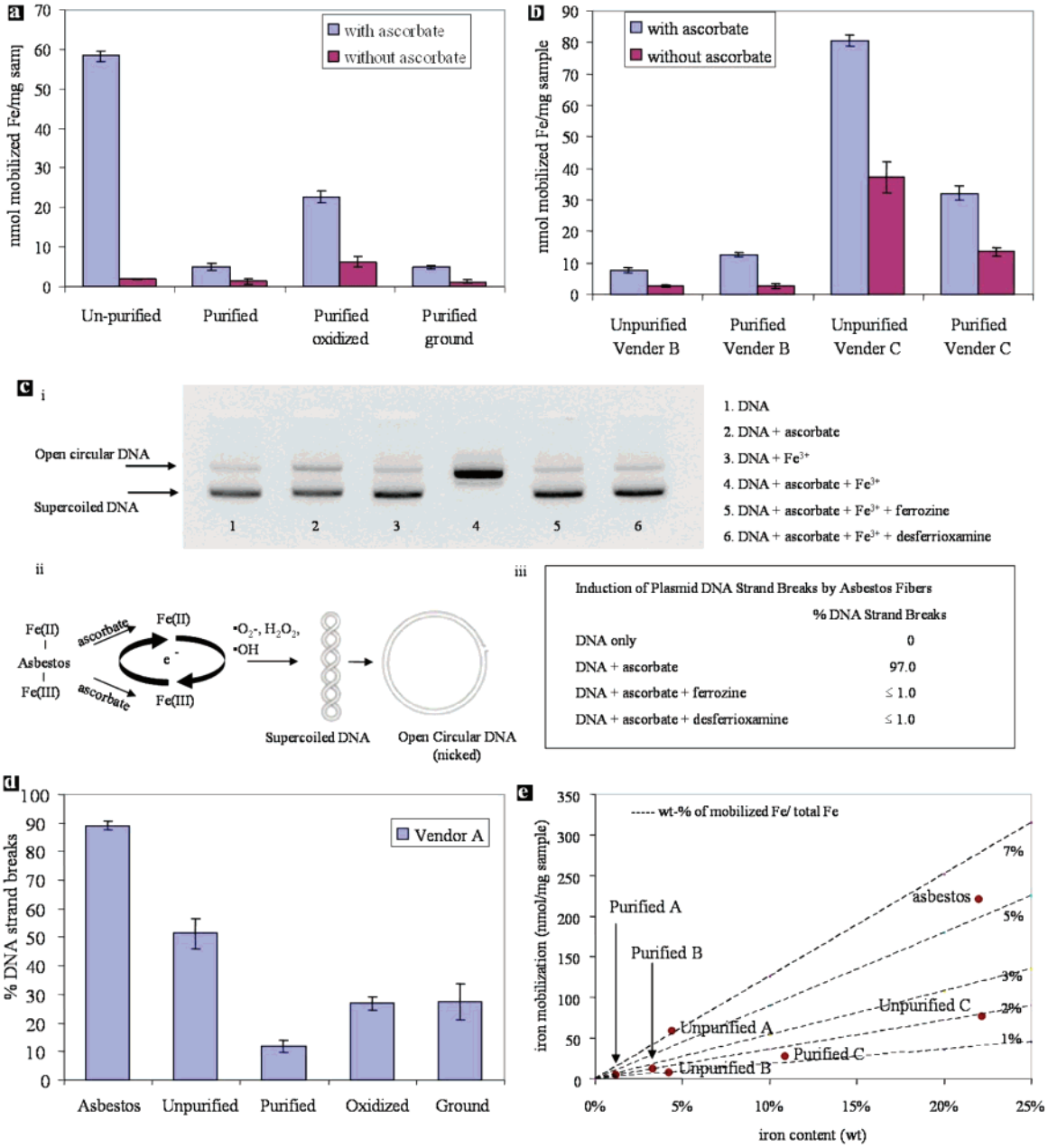

Figure 2. Results of mobilization and DNA breaks assays applied to commercial carbon nanotubes and reference materials. Panels (a) and (b) quantitate iron mobilized from eight commercial nanotube samples. Panel (a) focuses on samples from vendor A, which we subjected to grinding and oxidation to simulate harsh postprocessing. The observed effect of ascorbate is due to reduction of Fe(III) to Fe(II), allowing its spectrophotometric detection by the Fe(II)−ferrozine complex. Ascorbate may also promote iron mobilization by converting Fe(III) to the more soluble Fe(II) forms. Panel (c) illustrates the proposed mechanism[8] for DNA damage by mobilized redox-active iron using iron salts and asbestos as calibration and reference materials. Panel (d) gives the results of the plasmid DNA break assay applied to commercial nanotube samples and asbestos fibers as a positive control. These CNTs have about half the potency of asbestos; vendor purification reduces but does not eliminate this activity. Panel (e) summarizes the mobilization data and shows a poor correlation with bulk (total) iron content of these samples, and reveals that the absolute amount of mobilized iron represents from 1 to 7% of the total iron content of the sample. Thus most CNT metal (93−99%) does act as if encapsulated, but a small fraction is bioavailable and this fraction is sufficient to produce toxicologically significant effects through a continuous catalytic cycle involving mobilized free iron. Statistical analyses: the mean values for the DNA break assay and mobilization assay are given ± s.e. calculated from 3 to 7 independent experiments and p values compared using the two-way student t test.

of mobilized iron. For example, for the unpurified sample from vender C, the mobilized (soluble) iron decreased from 77.5 nmol/mg after 30 min of bath sonication at 100 W (our standard condition for this mobilization assay) to 63.5 nmol/mg when the sonication step was omitted. Vendor purification significantly reduced iron mobilization in two of three cases ($p < 0.001$), although even the purified materials still show measurable and in some cases significant Fe release. Intentional air oxidation to simulate harsh postprocessing increased iron mobilization significantly in the presence of ascorbate ($p < 0.01$, Figure 2b). The UICC crocidolite asbestos reference sample also released iron under these conditions as reported previously.[25]

Iron mobilized from asbestos fibers[26] or urban air particulates[27] can participate in iron-catalyzed Haber−Weiss reactions involving physiologic reductants including ascorbate, cysteine, or glutathione and the oxidants O_2 or H_2O_2.

(25) Lund, L. G.; Aust, A. E. *Biochem. Biophys.* **1990**, *278* (1), 60−64.
(26) Lund, L. G.; Aust, A. E. *Carcinogenesis* **1992**, *13*, 637−642.
(27) Smith, K. R.; Aust, A. E. *Chem. Res. Toxicol.* **1997**, *10*, 828−834.

Redox activity of iron mobilized from fibers or particulates was assessed here by measurement of the induction of DNA breaks in supercoiled plasmid DNA, as illustrated in Figure 2c. Induction of plasmid DNA breaks by $FeCl_3$ or crocidolite asbestos fibers required ascorbate, a physiologic reductant, and was prevented by the iron chelators ferrozine or desferrioxamine, which bind tightly to Fe^{2+} and Fe^{3+}, respectively, thus preventing redox cycling.[11] Under these conditions, redox active iron was mobilized into the supernatant following centrifugation to remove asbestos fibers[26] (Figure 2d). Similar to asbestos fibers, we found that the redox activity of iron mobilized by ascorbate from the commercial MWNT samples was completely inhibited by ferrozine or desferrioxamine. UICC asbestos fibers induced a higher percentage of DNA breaks than the unpurified sample from vendor A ($p < 3 \times 10^{-8}$). The purified samples that were postprocessed (oxidized or ground) were more active in inducing DNA breaks than the purified sample ($p < 0.009$), but all CNT samples showed significant DNA break percentages.

To better understand the behavior of iron in complex nanotube samples, we developed a model material system with well-defined and accessible surface iron in association with nanofibrous carbon. Figure 3 shows carbon nanofibers (CNFs) fabricated using a nanochannel alumina templating method employing a discotic liquid crystalline precursor.[21] These uniform diameter nanofibers provide a high-purity negative control material for this study and serve as the platform for surface iron doping. The doping procedure (see Methods) yielded zero-valent α-iron nanoparticles as determined by XRD (Figure 4) and the doping stoichiometry was chosen to give a total iron content of 5.7 wt %, which is similar to the commercial MWNT sample A. Figure 3 shows that these iron-doped nanofibers gave higher activities than the commercial CVD nanotubes in both the iron mobilization assay and the plasmid DNA single-strand break assay, which we propose reflects the high degree of accessibility of surface-doped iron nanoparticles relative to the partially encapsulated iron in CVD nanotubes.

The model Fe/C nanomaterial system also allowed a systematic study of sample aging, phase, and oxidation effects. Figure 4 shows that iron mobilization varies dramatically with age over the course of 1 year, passing through a maximum as a function of storage time in air-filled vials at ambient temperature. Zero-valent iron nanoparticles used in other applications are known to be unstable to oxidation in the presence of molecular oxygen in the gas-phase[28,29] or in aqueous solution.[30,31] The XRD spectra in Figure 4 show a large decrease in the zero-valent α-Fe phase and an increase in oxide phases during the first 4 months. Accelerated oxidation by air calcining for 10 min at temperatures from 250−450 °C significantly reduces iron mobilization in a way that parallels the aging effect (see inset). For comparison,

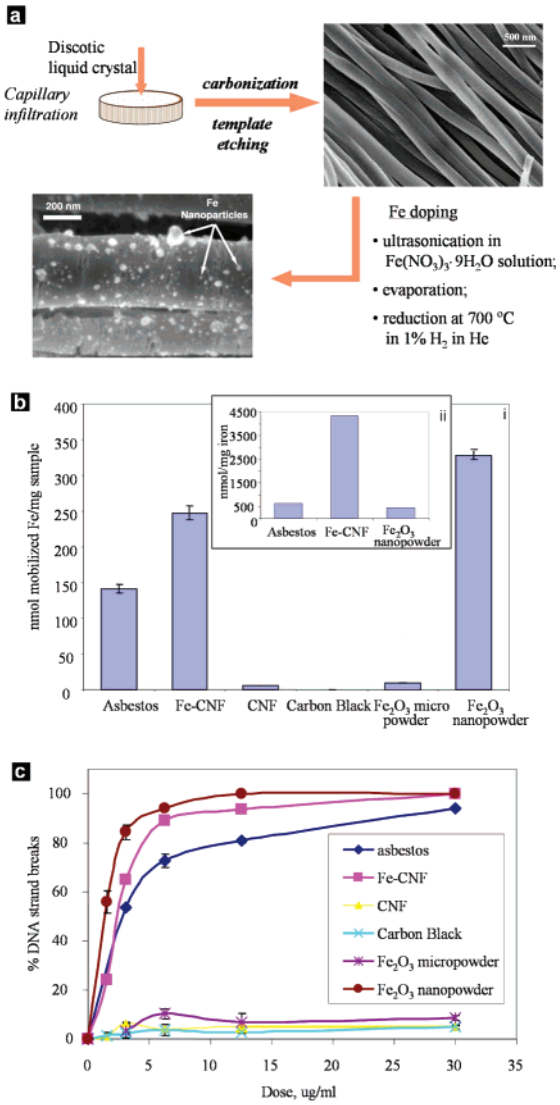

Figure 3. Results of mobilization and DNA break assay applied to diverse Fe, C, and Fe/C model materials. Panel (a) outlines the in-house synthesis of carbon nanofibers[21] (CNF) and the iron doping procedure that leads to highly accessible, surface-bound, nanophase iron in association with the CNFs. Panel (b) shows the results of the iron mobilization assay for a range of these model materials. Noteworthy is the high activity of the surface-doped fully accessible iron (Fe−CNF), which exceeds that of asbestos and is three times higher than the highest of the commercial CNTs samples in Figure 1. Note that the iron content of these samples varies greatly, so the data have also been presented in the inset to reflect mobilization per unit mass of Fe in the sample. The large specific iron release from the accessible, surface-doped reduced iron (Fe−CNF) is particularly apparent in the inset. Panel (c) shows dose−response curves for the plasmid DNA break assay for a variety of Fe-containing model materials and reference materials. The plots show strong influence of the iron phase and particle size on the ability of these solid materials to induce single-strand DNA breaks. Low activities are seen for the undoped negative reference materials (carbon nanofibers and carbon black), a result that clearly implicates iron as the cause of the majority of the DNA break activity. Low activity is also seen for fully oxidized iron particles (Fe_2O_3) in the form of conventional micrometer-scale powder. The corresponding nanophase powder has much higher activity, similar to asbestos and Fe-doped carbon nanofibers. Note, however, that the Fe_2O_3 nanopowder is introduced without carbon and thus has a much higher elemental Fe content (70%) than either asbestos (22.2%) or the Fe-doped CNFs (5.7 wt %). Statistical analyses: the mean values ± s.e. were calculated from 3 to 7 independent experiments and p values compared using the two-way student t test.

commercial Fe_2O_3 nanoparticles have a relatively low mobilization activity (on a unit mass of Fe basis), consistent with the thermodynamic stability of Fe_2O_3.

(28) Smits, J.; Bincheski, B.; Namkung, M.; Crooks, R.; Louie, R. *Mater. Sci. Eng., A* **2003**, *358*, 384−389.
(29) Signorini, L.; Pasquini, L.; Boscherini, F.; Bonetti, E. *Phys. Rev. B* **2003**, *68*, 195423.
(30) Zhang, W. *J. Nanopart. Res.* **2003**, *5*, 323−332.
(31) Kanel, S. R.; Manning, B.; Charlet, L.; Choi, H. *Environ. Sci. Technol.* **2005**, *39*, 1291−1298.

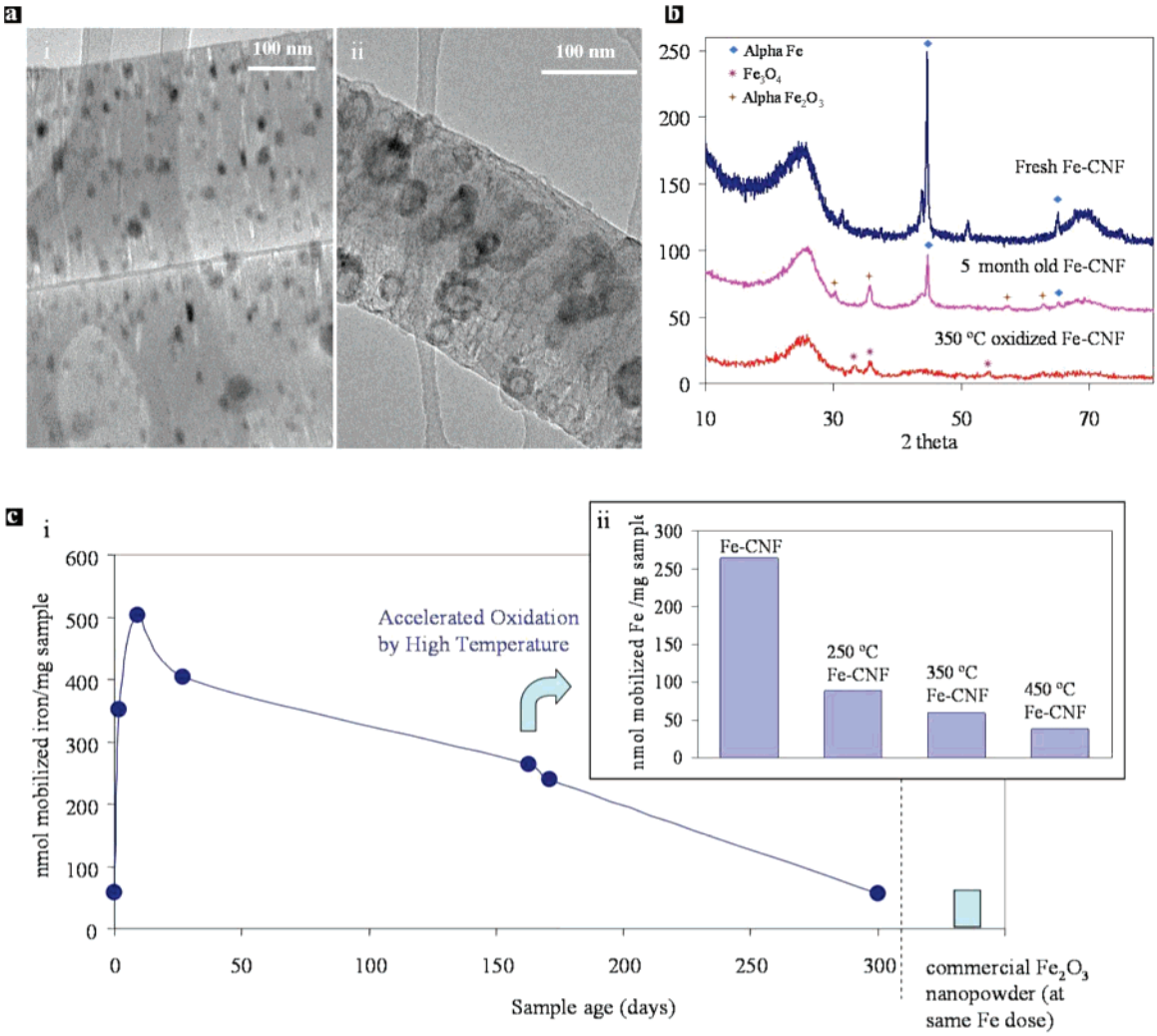

Figure 4. Effect of sample aging and thermal air oxidation on the bioavailability of iron in the model Fe/C nanofibers. (a) TEM images of Fe-doped CNFs as-produced (left) and after 10 min air oxidization at 350 °C, (b) XRD spectra of as-produced, aged, and air-oxidized samples, (c) results of Fe-mobilization assay as a function of age (main plot) and thermal air oxidation (inset) starting with the 160 day sample. The first data point in panel c was obtained by transferring the CNT−Fe samples directly from the H_2/He catalyst reduction environment into nitrogen-flushed vials to avoid atmospheric exposure.

The relatively low activity of very "fresh" iron (<7 days) is an interesting feature of our data (Figure 4c). Iron mobilization requires oxidation to a soluble form, which can occur either during the aqueous-phase assay or prior to the assay through atmospheric exposure. The reaction between nanoscale zero-valent iron and dissolved dioxygen is reported to be kinetically limited with full oxidation reported after 60 days[31] and retention of at least some reducing power up to 50 days in groundwaters.[30] The present results indicate that the early stages of oxidation in the atmosphere accelerate subsequent mobilization in solution and thus increase iron bioavailability and potential redox-mediated toxicity. Further oxidation eventually leads to formation of the more stable Fe_3O_4 or Fe_2O_3 phases and corresponding decreases in mobilization in the time range 10−300 days.

Discussion

The early literature on nanotoxicology describes significant variability in the biological response to CNTs[1−7,19] and work is now underway in many laboratories to identify the mechanisms and material properties responsible for this variability. The high iron content in some CNTs (up to 20% as produced and up to 10% in purified varieties) as well as the reducing conditions during synthesis create the potential for Fe-induced toxicity, but the complex Fe/C association morphologies dominated by apparent carbon encapsulation make its release characteristics uncertain and a possible source of variability. The biochemical mechanisms of iron-induced oxidative stress have been extensively studied,[18] but the knowledge base acquired in these studies cannot be directly applied in the case of nanotube exposure without knowledge of the material-specific iron-release characteristic of these unique materials. Our goal therefore was to systematically quantify the bioavailability of CNT iron for a variety of sample types and processing histories.

A 3-day exposure in the presence of the chelating agent ferrozine mobilizes iron for each of the commercial samples in a manner that varies greatly among samples and does not correlate directly with total bulk iron content. The iron is released in a redox-active soluble form, and even the vendor "purified" materials continue to release measurable amounts of iron. For these reasons, it is not sufficient in nanotoxicology studies to identify CNT samples only by the labels "as-produced" or "purified," nor to report total Fe by standard

elemental analysis. A specific assay for free, or bioavailable, iron is desirable for the complete characterization of CNTs used in biological applications. As an aside, it is worth noting that purification may influence toxicity by mechanisms unrelated to metal bioavailability. For example, acid washing may also introduce functional groups on nanotube surfaces, which in turn may affect solubility, material distribution, and partitioning in complex biological environments, and cytotoxicity.[7] The extent of iron release represents from 1 to 7% of the total iron, which is up to half of the iron mobilized from crocidolite asbestos used as a reference material (78 vs 150 nmol Fe/mg of sample). These results helps reconcile two opposing viewpoints on CNT metals. The first viewpoint, held by some researchers involved in CNT synthesis and manufacturing, is that the metals are fully encapsulated, a viewpoint that is based on electron microscopy as well as the common observation that oxidation is required to damage the carbon shells before significant quantities of metal can be removed by acid treatment. The second viewpoint, held by some toxicologists, is that iron must be bioavailable to explain Fe-induced oxidative stress and lipid peroxidation observed in recent cell culture studies.[4] The present results make it clear that most of the iron is indeed encapsulated (93−99% not mobilized in a 3-day assay in the presence of strong chelators), but a small fraction is fluid accessible and that fraction is sufficient to release toxicologically relevant amounts of iron and drive redox reactions that cause DNA single-strand breaks at a rate less than but on the same order of magnitude as crocidolite asbestos (Figure 2).

All three postprocessing stresses examined, oxidation, mechanical grinding, and sonication, modestly enhance Fe release. It has been suggested that sonication may damage carbon shells and allow or facilitate release of metal.[16] These results and a parallel study on nickel[32] both show that sonication does indeed promote metal release, but the effect is only a modest enhancement; most of the release in these two studies occurs even when the sonication step is omitted, implying that some fraction of the metal is intrinsically fluid accessible. Metal-induced toxicity cannot be suppressed by simply avoiding sonication.

The present results also suggest that CNT sample age is an important variable in toxicity. Our custom synthesized Fe/C nanofiber model system shows dramatic variation in Fe mobilization over the course of 1-year atmospheric exposure due to progressive oxidation. We anticipate that the small fraction of iron that is accessible in catalytically grown nanotubes undergoes a similar aging process and that this heretofore undocumented aging effect can lead to complex and time-dependent CNT toxicity profiles that may contribute to variability and inconsistency between data sets in the current CNT toxicology literature.

An important question is why vendor purification reduces Fe bioavailability in only two of three cases, and why none of the vendor purification processes successfully eliminates detectable bioavailable iron. Many purification procedures are proprietary, but common schemes use oxidizing acids (e.g., HNO_3), which attack both carbon shells and metal particles, followed by air oxidation to remove amorphous carbon.[33] On the basis of our results (Figure 2a) we predict that a final air oxidation step would expose additional metal and give the "purified" product a finite metal bioavailability. Another common purification method is air oxidation followed by treatment with non-oxidizing acids, and in this case, the origin of bioavailable metal is not obvious, as the final acid washing would be expected to access any exposed metal. Possible sources are deposited salt films or ion-exchanged cations that were not completely removed by washing following the acid dissolution step.

Finally, we note that current purification techniques have not been designed to reduce CNT toxicity, but rather to remove as much of the total metal and amorphous carbon as possible and thereby increase the CNT fraction in the final product. A significant challenge for purification strategies is to liberate metal by carbon shell damage without causing oxidative damage to the CNTs themselves, and the resulting compromise is responsible for the total metal content in the "purified" materials. Because the present results show that only a small portion of the total metal in nanotubes is bioavailable, a practical approach for reducing CNT health impacts may be not to target the total metal, but rather selectively remove or passivate only the bioavailable portion in a manner that does not damage the nanotubes. As a first proof of principle, we have incubated the purified CNT sample from vendor C, which despite the vendor's efforts still shows significant iron mobilization (Figure 2), with strong iron chelators to remove and deactivate the bioavailable iron. Treatment with 10 mM desferrioxamine for 17 h at room temperature followed by six water washes reduced subsequent Fe mobilization from 32.0 to 3.8 nmol Fe/mg of CNT ($p < 0.001$). The same treatment with a cocktail of 10 mM desferrioxamine and 10 mmol ferrozine reduced iron mobilization from 32.0 to 0.87 nmol/mg ($p < 0.001$). This result demonstrates the potential to minimize nanotube health risks by development of less invasive purification schemes that selectively target the bioavailable portion of CNT catalyst residues.

Acknowledgment. Financial support was provided by EPA STAR Grant RD-83171901-0 and the Superfund Basic Research Program Grant P42 ES013660. We acknowledge William Reiff for the Mössbauer analysis, Kengqing Jian and Margaret Tsien at Brown for technical support, and Zhijin Wu at Brown for statistical analyses. Although the research described in the article has been funded by the EPA and NIEHS, it does not necessarily reflect the views of either Agency, and no official dorsement should be inferred.

CM062691P

(32) Liu, X.; Kane, A.; Hurt, R. H. *Prepr. Pap.—Am. Chem. Soc., Div. Fuel. Chem.* Fall 2006 National Meeting. Gurel, V.; Morris, D.; Murray, D.; Zhitkovich, A.; Kane, A. B.; Hurt, R. H. Bioavailability of Nickel in Single-Wall carbon Nanotubes. *Adv. Mater.*; in press.

(33) Martinez, M. T.; Callejas, M. A.; Benito, A. M.; Cochet, M.; Seeger, T.; Anson, A.; Schreiber, J.; Gordon, C.; Marhic, C.; Chauvet, O.; Maser, W. K. *Nanotechnology* **2003**, *14*, 691−695.